Nanocrystal Formation

DOI: 10.1002/anie.201304958

The Formation Mechanism of Binary Semiconductor Nanomaterials: Shared by Single-Source and Dual-Source Precursor Approaches**

Kui Yu, Xiangyang Liu, Qun Zeng, Mingli Yang,* Jianying Ouyang, Xinqin Wang, and Ye Tao*

Semiconductor materials are technologically important and impact our daily lives in various aspects.[1–9] Both single-source and dual-source precursor approaches (SSPA and DSPA) to binary semiconductors have been documented.[9–27] Such materials consist of elements from two groups such as IIB and VIA. The single-source precursors (SSPs) consist of the metallic and nonmetallic elements of the semiconductor constituents in a single molecule.[9–14] DSPA uses separated metallic-element and nonmetallic-element precursors, which commonly involve metal carboxylates ($M(OOCR)_n$ such as M = Zn, Cd, Pb, Cu, In) and phosphine chalcogenides (such as $E=PHR_2$ where E = S, Se, Te),[15–27] respectively. Despite the large number of recipes developed for the various colloidal semiconductor nanocrystals (NCs) in the past 20 years, there is still little understanding of their formation mechanisms. To realize the full potential of semiconductor materials, there is an urgent need to advance our mechanistic understanding. Filling this gap in our knowledge should have practical implications such as lowering the high temperature currently employed for syntheses and offering new avenues to optimize the design of low-temperature approaches to novel semiconductor nanomaterials.

Recent evidence suggests that the formation of various binary semiconductor NCs by SSPAs and DSPAs may share analogous mechanisms. A DSPA to CdS quantumm dots (QDs) at 160 °C in tetradecane ($CH_3(CH_2)_{12}CH_3$) was reported from the reaction of cadmium stearate ($Cd(OOCC_{17}H_{35})_2$) and diphenylphosphine sulfide ($S=PHPh_2$).[25] DSAPs to E-based semiconductor QDs have become popular with metal carboxylates as cation precursors and diphenylphosphine chalcogenides $E=PHPh_2$ as anion precursors.[15–27] Astonishingly, the lack of a common formation mechanism is actually accompanied by the same ^{31}P NMR identification of $RCOO\text{-}PPh_2$ (R = $C_{17}H_{33}$ 99 ppm (**3** in Scheme 1) or C_6H_5 102 ppm) and $Ph_2P\text{-}PPh_2$ (−14 ppm, **4**) for the various DSPAs to PbSe,[18] CdSe,[19–22] ZnSe,[23,24] ZnS,[24] and ZnSeS,[24] together with $C_{17}H_{33}COO\text{-}P(Se)Ph_2$ (77 ppm, **5**) for the Se-based NCs.[18,21–24] Furthermore, the conversion of $Se=PHPh_2$ to diphenyldiselenophosphinate derivatives ($-SeSePPh_2$) has been documented.[18,19,22] For instance,[22] the formation of $RCOOCdSeSePPh_2$ (**c**) was proposed from a $Cd(OA)_2$ + $Se=PHPh_2$ reaction after the release of oleic acid ($C_{17}H_{33}COOH$ or RCOOH, R = $C_{17}H_{33}$) from $(RCOO)_2Cd(Se=PHPh_2)_2$ (**b**) followed by diphenylphosphine ($HPPh_2$ or DPP) from $RCOOCd(Se-PPh_2)\text{-}(Se=PHPh_2)$ (**d**) through cleavage of the Se=P bond of the $Se=PHPh_2$ coordination arm.

Recently, a SSP, cadmium bis(diphenyldithiophosphinate) ($Cd(SSPPh_2)_2$), together with cadmium oleate $Cd(OA)_2$, was used to synthesize CdS QDs at 240 °C in 1-octadecene (ODE).[14] Without $Cd(OA)_2$, $Cd(SSPPh_2)_2$ did not produce CdS QDs at 240 °C. Various dithiophosphinato or diselenophosphinato complexes have been synthesized, with the general structures of $M(EEPR_2)_n$, where M = metal ions of Group IIIA (trivalent), IIB (divalent), IVA (divalent), and IB (monovalent), and R = alkyl, phenyl, and alkoxy groups.[28–32] Some of these complexes have been used in SSPAs to make E-based binary semiconductor NCs and thin films but only at temperature higher than 300 °C.[9–14]

To explore the common mechanism for the formation of the various ME semiconductor nanomaterials from the SSPA and DSPA, herein, CdSe was investigated as a model system in detail. ^{31}P NMR spectroscopy was used to monitor key products involved in the formation of CdSe NCs from the SSPA and DSPA which we have designed. As shown in Scheme 1, the former addresses the reaction of cadium bis(diphenyldiselenophosphinate) [$Cd(SeSePPh_2)_2$] (**2**) in ODE, in the presence of $Cd(OA)_2$ and DPP. The latter deals with the $Cd(OA)_2$ + SeDPP reaction in ODE. Also, in situ absorption was used to monitor the formation of NCs and density functional theory (DFT) calculations were performed to study the reactants, intermediates (IM), transition states (TS), and products. On the basis of the NMR spectroscopy, in situ absorption, and DFT calculations, we propose an essentially identical mechanism for the two approaches, as illustrated in Scheme 1 which seems to be complicated but can be understood readily with numerous metathesis equilibriums and Se exchange reactions.

Scheme 1 presents two manifolds of equilibriums, **c**, **d**, **e** and **3** (top), and **f**, **g**, **h**, and **4** (bottom). Simply, the top manifold leads to **3** and CdSe (clusters and NCs) (and **5**); the

[*] Dr. K. Yu, Dr. X. Liu, Dr. J. Ouyang, Dr. Y. Tao
National Research Council of Canada
Ottawa, ON, K1A 0R6 (Canada)
E-mail: kui.yu@nrc-cnrc.gc.ca
Q. Zeng, Prof. M. Yang, X. Wang
Institute of Atomic and Molecular Physics and State Key Laboratory of Biotherapy, Sichuan University
Chengdu 610065 (P. R. China)
E-mail: myang@scu.edu.cn

[**] K.Y. thanks Dr. Keith Ingold for valuable discussions and Dr. Danial Wayner for precious encouragement. The authors thanks Erik Huisman for some of the in situ absorption measurements presented and the Defence Research and Development Canada Centre for Security Science Chemical, Biological, Radiological/Nuclear, and Explosives Research and Technology Initiative (CRTI 09-0511RD "Next-generation stand-off radiation detection using nanosensors") for financial support.

Supporting information for this article is available on the WWW under http://dx.doi.org/10.1002/anie.201304958.

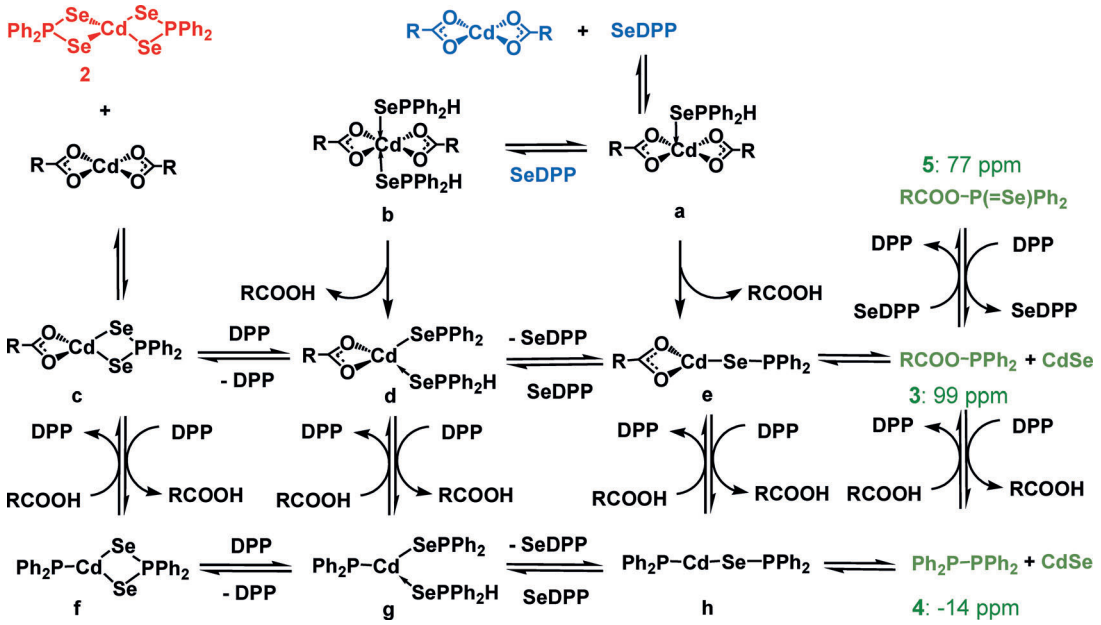

Scheme 1. The reaction mechanism proposed for the SSPA (red) and DSPA (blue) with $Cd(SeSePPh_2)_2$ (**2**) and $Cd(OA)_2$ + SeDPP, respectively. This mechanism include the metathesis reactions of x + DPP ⇄ y + RCOOH, where x/y = **c**/**f**, **d**/**g**, **e**/**h**, and **3**/**4**, and the Se exchange reaction between **3**/**5**. The formation of $(CdSe)_n$ clusters drives the equilibriums to the products (green). The compounds labeled by numbers were detected by ^{31}P NMR spectroscopy and summarized in Table S1, and those labeled by letters were studied by DFT (Schemes S2–S5).

bottom manifold results in **4** and CdSe (cluters and NCs). The Se exchange reaction between **3** and **5** [Supporting Information, Scheme S1, Eq. (6)], **3** + SeDPP ⇄ **5** + DPP, is similar to TOP + SeDPP ⇄ TOPSe + DPP.[18,22] The top and bottom manifolds are connected by the four metathesis reactions which involve the reversible exchange of $HPPh_2$ and $C_{17}H_{33}COOH$ between **c** and **f**, **d** and **g**, **e** and **h**, and **3** and **4** [Scheme S1, Eq. (1) to (4)]. The mechanism proposed is in full agreement with our experimental observations: both the SSAP and DSAP lead to the same products, which are the three phosphorus-containing compounds (**3**, **4**, and **5**) and CdSe NCs.

Furthermore, the feed molar ratio of the reactants affects the relative amounts of the three phosphorus-containing compounds obtained and the amount and size of the CdSe NCs. RCOOH and DPP favor the top and bottom manifolds, respectively. The formation of the CdSe NCs is thermodynamically favored, which shifts the equilibriums to the products. While Compounds **3**, **4**, and **5** have been previously monitored by ^{31}P NMR spectroscopy from the various DSPAs,[18–24] the present study provides a common mechanism for their formation from the DSPA with $M(OOCR)_n$ and E = $PHPh_2$ and from the SSPA with $M(EEPPh_2)_n$. With far-reaching implications, our findings delineate the fundamental understanding of the formation mechanism and endorse subsequently the low-temperature design and syntheses of various binary and alloyed NCs, bringing insight to the empirical use of additives such as $M(OOCR)_n$, DPP, and RCOOH as a means to promote low-temperature syntheses (particularly for the SSPA).

Figure 1 shows ^{31}P NMR spectra of the SSPA and DSPA at room temperature of **2** + $Cd(OA)_2$ + DPP (a–c) and $Cd(OA)_2$ + SeDPP (d–f), respectively. Compound **2** is $Cd(SeSePPh_2)_2$. For the former approach, 0.005 mmol of **2** was used. For the latter approach, the amount of its limiting reactants was 0.03 mmol. The collected ^{31}P NMR spectra are fairly similar. Compounds **3**, **4**, and **5** were obtained from the both approaches and appear to share similar or identical reaction pathways, as proposed in Scheme 1.

Moreover, an increase in the amount of $Cd(OA)_2$ increases the **3**-to-**4** ratio for the both approaches. For the **2** + 14 $Cd(OA)_2$ + 1 DPP reaction (a), a small amount of **4** and a large amount of **3** were observed, similar to the 2 $Cd(OA)_2$ + 1 SeDPP reaction (d). For the **2** + 1 $Cd(OA)_2$ + 1 DPP reaction (c), a large amount of **4** and a tiny amount of **3** were observed, similar to the 1 $Cd(OA)_2$ + 3 SeDPP reaction (f). Due to the equilibrium of **3** + DPP ⇄ **4** + RCOOH weighted toward the left (Figure S1a), the formation of the large amount of **4** (particularly during the proceeding of Reaction c) should be mainly from **h** instead of **3**.

A significant amount of **5** was obtained in reactions (b) and (e) (Figure 1), but almost no **5** was detected in reactions (c) and (f) (with the relatively small Cd-to-Se feed molar ratios) and in reactions (a) and (d) (with the relatively large Cd-to-Se feed molar ratios). Such observations can be readily understood by the fact that the reaction of $Cd(OA)_2$ and SeDPP is astonishingly fast (even at −55 °C),[22] while the equilibrium of **3** + SeDPP ⇄ **5** + DPP is weighted toward the right (Figure S1a), similar to that of TOP + SeDPP ⇄ SeTOP + DPP.[30,31] When $Cd(OA)_2$ is in excess (reactions (a) and (d)), SeDPP (such as released from **d** in the SSPA) should react with $Cd(OA)_2$ instead of **3** and little **5** could be obtained. When $Cd(OA)_2$ is not excess (reactions (b) and (e)), SeDPP could react with **3** and an apparent amount of **5** could be obtained. Thus, the fact, that the Cd-to-Se feed molar ratio affects the relative amount of compounds **3**, **4**, and **5**, supports

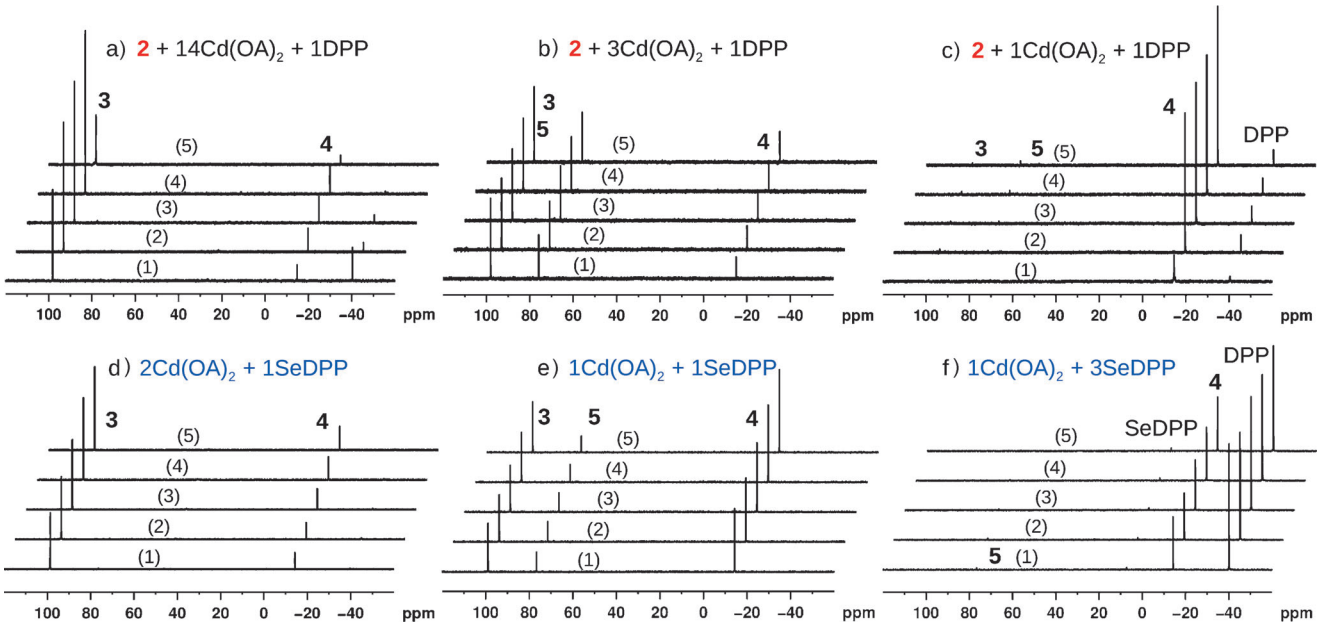

Figure 1. ^{31}P NMR study of the SSPA of the three reactions of **2** in the presence of $Cd(OA)_2$ and DPP (a–c) and the DSPA of the three reactions of $Cd(OA)_2$ + SeDPP (d–f). The spectra were collected at room temperature with each reaction proceeding at 5 min (1), 10 min (2), 20 min (3), 40 min (4), and 60 min (5). Compounds **3**, **4**, and **5** were obtained from the two approaches, with high Cd-to-Se feed molar ratios promoting the **3**-to-**4** ratio.

also the chemical mechanism illustrated by Scheme 1. Also, the effect of such ratios on the nucleation and growth of CdSe NCs appear analogous for the two approaches (Figure S1b).

The synthesis and characterization of **2** is illustrated in Figure S1c. The dispersion of purified **2** in toluene was stable with a chemical shift of 12.0 ppm and $J_{P\text{-}Se}$ of 480 Hz at 100 °C and no obvious decomposition was detected over 2 h. In the presence of $Cd(OA)_2$, the disappearance of **2** in toluene at 80 °C led to a clear solution, and a phosphorus resonance at 16.2 ppm and $J_{P\text{-}Se}$ of 496 Hz at 100 °C was detected and assigned to $C_{17}H_{33}COO\text{-}Cd\text{-}SeSePPh_2$ (**c**). In the presence of DPP and/or RCOOH, purified **2** in toluene/ODE remained (as a white solid) even at 80 °C, with only a small amount of SeDPP and **4** detected. In the presence of both $Cd(OA)_2$ and DPP, the reactivity of **2** in ODE increased profoundly at temperature as low as 50 °C (Figure S1c-4); the presence of both $Cd(OA)_2$ and DPP is important for the SSPA to CdSe NCs.

Figure 2 shows the increase of **4** from **h** by DPP and **3** from **e** by RCOOH. The ^{31}P NMR spectra were collected from the SSPA of **2** + 6 $Cd(OA)_2$ + x DPP (top) and **2** + 6 $Cd(OA)_2$ + x DPP + 1 RCOOH (bottom) reactions at room temperature, with $x = 0.5$ (a and b), 1 (c and d), and 4 (e and f). Again, 0.005 mmol of Compound **2** was used. From 0.5 DPP to 4 DPP, the **3**-to-**4** ratio decreases together with the disappearance of **5**. Along the proceeding of reactions (e) and (f) with 4 DPP, the significant increase of **4** indicates evidently its foremost formation from **h** instead of **3**. Thus, DPP seems to promote the formation of **4** from **h** together with the suppression of **5** from **3** + SeDPP ⇄ **5** + DPP. For reactions (c) and (d) with 1 DPP, reaction (d) produced more **3** and **5** at its early stage than reaction (c) did. Clearly, reaction (d) (with 1 RCOOH) suppressed **4** and promoted **3** (and thus **5**). Along the proceeding of reaction (d), the remarkable increase of **3** in the presence of a tiny amount of **4** specifies outstandingly the probable formation of **3** from **e** (instead of **4**). The effect of DPP on the promotion of **4** and the effect of RCOOH on the promotion of **3** support the chemical mechanism illustrated in Scheme 1.

Figure S2 demonstrates the enhanced nucleation and growth of CdSe NCs from the SSPA by DPP and RCOOH. Obviously, the increase of DPP (top, **2** + 6 $Cd(OA)_2$ + x DPP + 1.2 OA with $x = 0.1$ and 0.2) and the increase of RCOOH (bottom, **2** + 6 $Cd(OA)_2$ + 1 DPP + (1.2 + y) OA with $y = 0$ and 0.8) increased the particle number. Note that RCOOH and DPP were released from the DSPA even at −55 °C;[22] thus, it is easy to understand that the effect of DPP and RCOOH may not be obvious for the DSPA (Figure S2).

Now, let us turn our attention to the reactions involving $HPPh_2$ shown in Scheme 1 such as **c** + $HPPh_2$. Two pathways shown in Scheme 2 are proposed, namely route I (**c** to **d**) and route II (**c** to **f**). Route I, a reversed process of the release of $HPPh_2$ from **d** leading to **c**,[22] was studied by DFT. Again, the CH_3 group was used to mimic the phenyl and $C_{17}H_{33}$ groups in our DFT calculations, such as dimetyl phosphine (DMP or $HPMe_2$) for DPP.[22] As computed in Scheme S2, the P atom of $HPMe_2$ attacks the Se atom of **c** leading to the formation of IM1 (Gibbs free energy $\Delta G = +33.6$ kJ mol^{-1}). Then, a new Se−P bond forms between $HPMe_2$ and **c**, while its neighboring Se−P bond is weakened, leading to TS1 ($\Delta G = +76.0$ kJ mol^{-1}) and subsequently **d** ($\Delta G = +50.0$ kJ mol^{-1}). Note that our DFT calculations were carried out at 298 K, producing similar results with TPSSh, TPSS, and B3LYP functionals. Although both total energy (ΔE) and ΔG variations were computed, only the values of ΔG from the

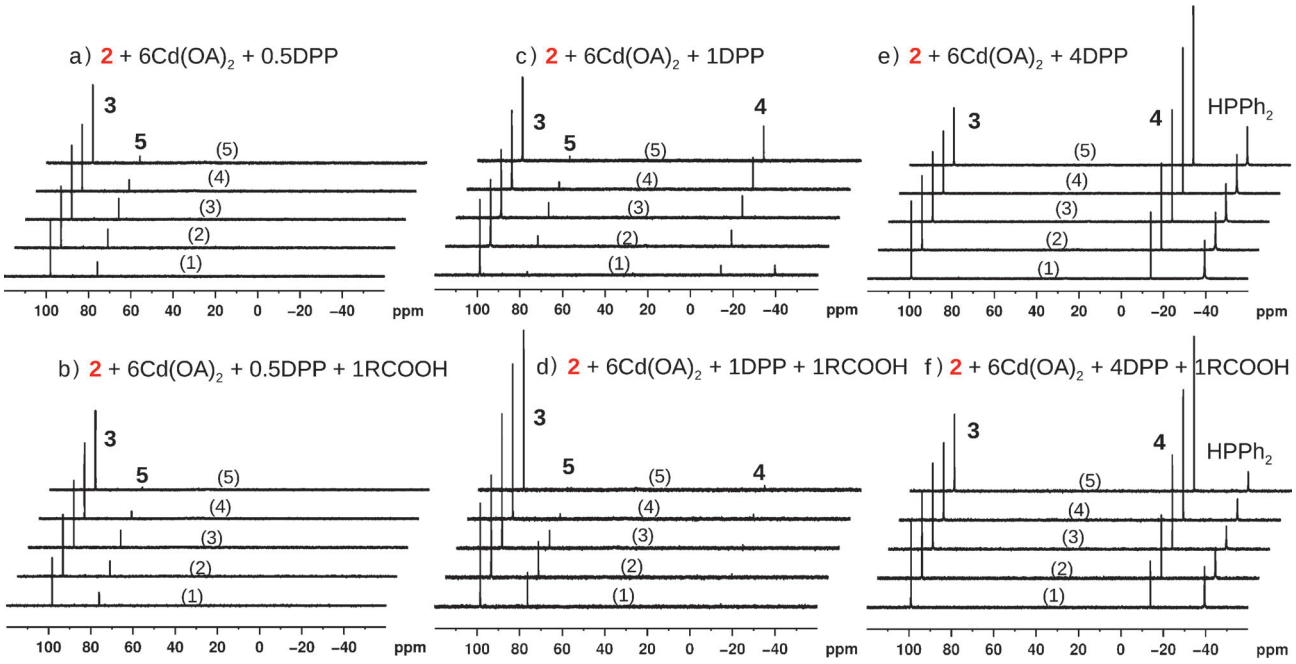

Figure 2. The effect of DPP and RCOOH studied by ^{31}P NMR spectroscopy. The spectra were collected at room temperature with each of the six reactions proceeding at 5 min (1), 10 min (2), 20 min (3), 40 min (4), and 60 min (5). Evidently, DPP promotes the formation of **4**, while oleic acid (RCOOH) assists the formation of **3**.

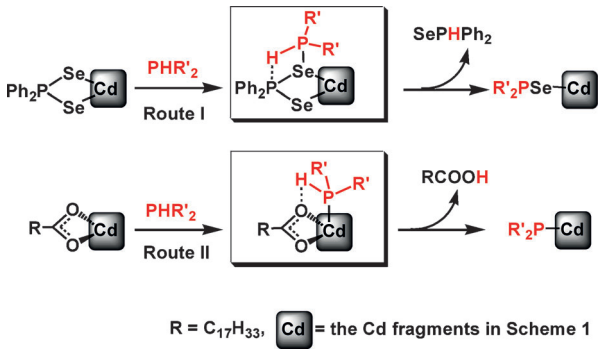

Scheme 2. Two reaction pathways proposed for $HPPh_2$ (where R′ = Ph_2). Route I (top) illustrates the interaction of P and Se for **c** to **d** and **f** to **g**. Route II (bottom) illustrates the interaction of P and Cd for **c** to **f**, **d** to **g**, and **e** to **h**; this pathway is substitution/metathesis.

TPSSh results are addressed, as the reactions took place at a constant temperature and pressure.

To exam route I further, we designed three reactions. Figure 3 shows in situ ^{31}P NMR spectra of the reactions of **2** + $HPPh_2$ in DMSO (dimethyl sulfoxide) (a), **2** + $HPCy_2$ (dicyclohexyl phospine) in ODE (b), and SeDPP + $HPCy_2$ (c). The amounts of **2** were 0.0125 mmol (a) and 0.005 mmol (b), and that of SeDPP was 0.01 mmol (c). $HPCy_2$ seems to be more reactive than $HPPh_2$ towards **2**. This middle reaction completed in minutes at room temperature with the dissolution of **2** resulting in a clear solution. The chemical shift at 54.8 ppm with $J_{P\text{-}Se} = 484$ Hz is assigned to **2″** (Cd-$(SeSePCy_2)_2$). To confirm, we synthesized **1″** ($Cy_2PSeSeNH_3R$, R = $C_{18}H_{35}$) and **2″**, following the synthetic procedure to **1** and **2**, respectively, but with $HPCy_2$ instead of $HPPh_2$ (Figure S3a-1). With the PCy_2 group instead of the PPh_2 group, **1″** and **2″** are analogous of **1** and **2**, respectively.

The detection of $SePPh_2H$ from the **2** + $HPPh_2$ reaction, together with **2″**, $SePPh_2H$, and $SePCy_2H$ from the **2** + $HPCy_2$ reaction provided us extremely valuable information to comprehend route I. The observation of SeDPP from these two reactions suggests the probable breakage of Se–P bond of the -$SeSePPh_2$ group of **2**. Figure S3a-2 presents our proposed chemical mechanism for the formation of **2″** from the **2** + $HPCy_2$ reaction, which proceeds through a multi-step equilibrium process. The P atom of $HPCy_2$ attacks the Se atom of **2** resulting in the breakage of the original Se–P bond. Afterward, the release of SeDPP leads to the formation of –Cd–$SePCy_2$ species. $HPCy_2$ reacts with SeDPP resulting in $SeHPCy_2$ (Figure 3, bottom). $SePCy_2H$ sequentially reacts with the –Cd–$SePCy_2$ part to form a Cd($SeSePCy_2$) fragment.

Also, we designed two groups of reactions to support Scheme 1 proposed. They are the **2** + $Cd(OA)_2$ + $HPCy_2$ group (Figure S3b, left) and the $Cd(OA)_2$ + $SePCy_2H$ group (Figure S3b, right). Compounds **3**, **3″** ($C_{17}H_{33}COOPCy_2$, 134 ppm), **5**, and **5″** ($C_{17}H_{33}COOP(Se)Cy_2$, 116 ppm) were detected from the former, and compounds **3″** and **5″** from the latter.

For route II, the P atom of $HPPh_2$ interacts with the Cd atom.[22] As computed in Scheme S3a, the proton of $HPMe_2$ approaches one O atom of **c**, leading to the formation of IM3 ($\Delta G = +6.8$ kJ mol^{-1}). After going through a barrier of 65.5 kJ mol^{-1}, TS3 ($\Delta G = +72.3$ kJ mol^{-1}) is obtained, which has a six-membered ring with the breakage of one original O–Cd bond and the proton bridging the O and P atoms. The breakage of the original H–P bond results in the formation of IM4 ($\Delta G = +61.9$ kJ mol^{-1}). Then HOAc is released, together with the formation of **f** ($\Delta G = +53.1$ kJ mol^{-1}). Thus, our DFT

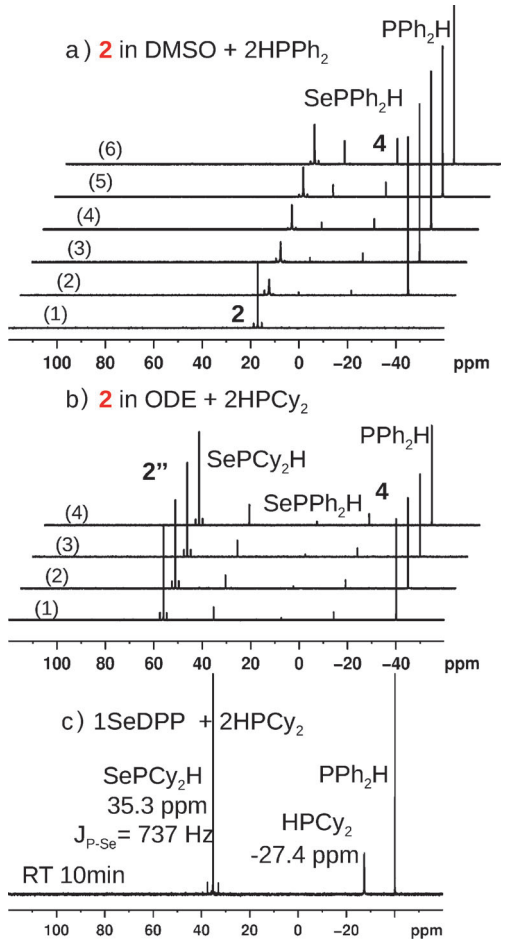

Figure 3. Three reactions with HPR_2 (where R = Ph (a) or Cy (b and c)) designed to investigate route I. a) The ^{31}P NMR spectra were in situ collected at room temperature before the addition of DPP (1), after the addition of DPP of 5 min (2), 10 min (3), 45 min (4), 120 min (5), and 210 min (6). b) the ^{31}P NMR spectra were obtained at 15 min (1) and 180 min (2) at room temperature, 30 min at 80 °C (3), and 30 min at 120 °C (4).

calculations demonstrate that routes I and II experience moderate energy barriers of 42.4 kJ mol^{-1} (TS1) and 65.5 kJ mol^{-1} (TS3), respectively, suggesting that the two routes are kinetically feasible at 298 K (room temperature).

For **d** → SeDPP + **e** (Scheme S2), the small increase in ΔG of 4.0 kJ mol^{-1} is worthy of notice, together with the small barrier of 7.8 kJ mol^{-1} (TS2). For **f** + DPP → **h** + SeDPP (Scheme S3b), the ΔG increase is 50.8 kJ mol^{-1} with a barrier of 54.2 kJ mol^{-1} (TS4). For **e** + DPP → **h** + HOAc (Scheme S4), the ΔG increase is 51.1 kJ mol^{-1} with a barrier of 82.5 kJ mol^{-1} (TS5). Thus, our DFT calculations suggest that **e** is both more thermodynamically and kinetically favored than **h**.

To test such a computational result, we designed two reactions, **2** + 3 $Cd(OA)_2$ + 3 $Cd(OOCPh_2)_2$ + 1 DPP (Figure S4 top) and **2** + 6 $Cd(OA)_2$ + 3 PhCOOH + 1 DPP (Figure S4 bottom). In addition to compounds **3** and **5**, compounds $PhCOOPPh_2$ (**3′**, 102 ppm) and $PhCOOP(Se)Ph_2$ (**5′**, 79 ppm) were also obtained, together with Ph_2P-PPh_2 (**4**, −14 ppm). Interestingly, similar amounts of **3** and **3′** were obtained from the top reaction, while a large amount of **3** and a tiny amount of **3′** were obtained from the bottom reaction. For the top reaction, thus, similar amounts of $C_{17}H_{33}COOCdSePPh_2$ (**e**) from $C_{17}H_{33}COOCdSeSePPh_2$ (**c**) and $PhCOOCdSePPh_2$ (**e′**) from $PhCOOCdSeSePPh_2$ (**c′**) should have formed. For the bottom reaction, the amount of **e** from **c** should be much more than that of **e′** from the reaction of $Ph_2PCdSePPh_2$ (**h**) + PhCOOH. Accordingly, the formation of **e** from **c** (through **d**) seems to be more favored than that of **h** from **c** (through **f** and **g**).

Finally, for the formation of $(CdSe)_n$ together with compounds **3** and **4** from **e** and **h**, respectively, the energy change is computed and summarized in Scheme S5. Intriguingly, ΔG is largely positive with $n = 1$, drops dramatically with $n = 2$, becomes negative with $n = 3$, and further decreases with $n = 6$ and 13. Thus, the formation of the $(CdSe)_n$ clusters ($n > 3$) lowers significantly the ΔG values; taking the ΔG of **c** as a reference, the total ΔG becomes negative with $n = 13$. Consequently, the formation of the $(CdSe)_n$ clusters are thermodynamically favored, driving the equilibriums to the product direction. The experimental observation of $(CdSe)_{13}$ (exhibiting the bandgap of ca. 350 nm) can be found elsewhere[33] and in Figure S1b and S2.

In conclusion, the present study addresses a significant gap in our understanding of the formation mechanism of semiconductor materials from the DSPA with $M(OOCR)_n$ and $E = PHPh_2$ and from the SSPA with $M(EEPPh_2)_n$. Based on our experimental data and DFT calculations, we have proposed a common chemical mechanism shared by the SSPA and DSPA to semiconductor nanomaterials. Also, the present study provides the fundamental insight for rational design and synthesis of semiconductor materials with enhanced particle yield at low reaction temperature. Collectively, the proposed mechanism suggests a set of design criteria to take advantage of the equilibriums, providing new avenues for low-temperature syntheses. Although our efforts focused on CdSe, the formation mechanism (Scheme 1) can be readily extended to other NC systems from the DSPA with $M(OOCR)_n$ and $E = PHPh_2$ and from the SSPA with $M(EEPPh_2)_n$.[9,18–24] We envision that the proposed mechanism should be broadly applicable to the design and synthesis of various binary and alloyed semiconductor materials. With new perspectives, the identification of the metathesis reactions should serve as a platform to improve our capability to engineer semiconductor materials with smarter approaches to satisfy the requirement on low-temperature syntheses with high quality.

Received: June 10, 2013
Published online: September 4, 2013

Keywords: metal–ligand interaction · molecular modeling · phosphines · nanocrystal formation mechanisms · semiconductor quantum dots

[1] S. Jun, E. Jang, *Angew. Chem.* **2013**, *125*, 707–710; *Angew. Chem. Int. Ed.* **2013**, *52*, 679–682.
[2] Y. Shirasaki, G. J. Supran, M. G. Bawendi, V. Bulovic, *Nat. Photonics* **2013**, *7*, 13–23.

[3] R. Gill, M. Zayats, I. Willner, *Angew. Chem.* **2008**, *120*, 7714 – 7736; *Angew. Chem. Int. Ed.* **2008**, *47*, 7602 – 7625.
[4] F. Song, P. S. Tang, H. Durst, D. T. Cramb, W. C. W. Chan, *Angew. Chem.* **2012**, *124*, 8903 – 8907; *Angew. Chem. Int. Ed.* **2012**, *51*, 8773 – 8777.
[5] E. H. Sargent, *Nat. Photonics* **2012**, *6*, 133 – 135.
[6] Q. H. Wang, K. Kalantar-Zadeh, A. Kis, J. N. Coleman, M. S. Strano, *Nat. Nanotechnol.* **2012**, *7*, 699 – 712.
[7] V. I. Klimov, A. A. Mikhailovsky, S. Xu, A. Malko, J. A. Hollingsworth, C. A. Leatherdale, H. Eisler, M. G. Bawendi, *Science* **2000**, *290*, 314 – 317.
[8] Z. Han, F. Qiu, R. Eisenberg, P. L. Holland, T. D. Krauss, *Science* **2012**, *338*, 1321 – 1324.
[9] M. A. Malik, M. Afzaal, P. O'Brien, *Chem. Rev.* **2010**, *110*, 4417 – 4446.
[10] J. Sun, W. E. Buhro, *Angew. Chem.* **2008**, *120*, 3259 – 3262; *Angew. Chem. Int. Ed.* **2008**, *47*, 3215 – 3218.
[11] C. Byrom, M. A. Malik, P. O'Brien, A. J. P. White, D. J. Williams, *Polyhedron* **2000**, *19*, 211 – 215.
[12] C. Q. Nguyen, M. Afzaal, M. A. Malik, M. Helliwell, J. Raftery, P. O'Brien, *J. Organomet. Chem.* **2007**, *692*, 2669 – 2677.
[13] N. O. Boadi, M. A. Malik, P. O'Brien, J. A. M. Awudza, *Dalton Trans.* **2012**, *41*, 10497 – 10506.
[14] M. P. Hendricks, B. M. Cossairt, J. S. Owen, *ACS Nano* **2012**, *6*, 10054 – 10062.
[15] M. R. Buck, R. E. Schaak, *Angew. Chem.* **2013**, *125*, 6270 – 6297; *Angew. Chem. Int. Ed.* **2013**, *52*, 6154 – 6178.
[16] L. De Trizio, M. Prato, A. Genovese, A. Casu, M. Povia, R. Simonutti, M. J. P. Alcocer, C. D'Andrea, F. Tassone, L. Manna, *Chem. Mater.* **2012**, *24*, 2400 – 2406.
[17] F. Wang, W. R. Buhro, *J. Am. Chem. Soc.* **2012**, *134*, 5369 – 5380.
[18] C. M. Evans, M. E. Evans, T. D. Krauss, *J. Am. Chem. Soc.* **2010**, *132*, 10973 – 10975.
[19] B. M. Cossairt, J. S. Owen, *Chem. Mater.* **2011**, *23*, 3114 – 3119.
[20] K. Yu, *Adv. Mater.* **2012**, *24*, 1123 – 1132.
[21] R. García-Rodríguez, H. Liu, *J. Am. Chem. Soc.* **2012**, *134*, 1400 – 1403.
[22] K. Yu, X. Liu, Q. Zeng, D. M. Leek, J. Ouyang, K. M. Whitmore, J. A. Ripmeester, Y. Tao, M. Yang, *Angew. Chem.* **2013**, *125*, 4923 – 4928; *Angew. Chem. Int. Ed.* **2013**, *52*, 4823 – 4828.
[23] K. Yu, A. Hrdina, X. Zhang, J. Ouyang, D. M. Leek, X. Wu, M. Gong, D. Wilkinson, C. Li, *Chem. Commun.* **2011**, *47*, 8811 – 8813.
[24] K. Yu, A. Hrdina, J. Ouyang, D. Kingston, X. Wu, D. M. Leek, X. Liu, C. Li, *ACS Appl. Mater. Interfaces* **2012**, *4*, 4302 – 4311.
[25] H. H.-Y. Wei, C. M. Evans, B. D. Swartz, A. J. Neukirch, J. Young, O. V. Prezhdo, T. D. Krauss, *Nano Lett.* **2012**, *12*, 4465 – 4471.
[26] K. Yu, J. Ouyang, D. M. Leek, *Small* **2011**, *7*, 2250 – 2262.
[27] See Supporting Information: K. Yu, et al., *ACS Appl. Mater. Interfaces* **2013**, *5*, 2870 – 2880.
[28] W. Kuchen, H. Hertel, *Angew. Chem.* **1969**, *81*, 127 – 135; *Angew. Chem. Int. Ed. Engl.* **1969**, *8*, 89 – 97.
[29] R. G. Cavell, E. D. Day, W. Byers, P. M. Watkins, *Inorg. Chem.* **1972**, *11*, 1759 – 1772.
[30] R. P. Davies, C. V. Francis, A. P. S. Jurd, M. G. Martinelli, A. J. P. White, D. J. Williams, *Inorg. Chem.* **2004**, *43*, 4802 – 4804.
[31] C. Q. Nguyen, A. Adeogun, M. Afzaal, M. A. Malik, P. O'Brien, *Chem. Commun.* **2006**, 2182 – 2184.
[32] P. K. Liao, D. R. Shi, J. H. Liao, C. W. Liu, A. V. Artem'ev, V. A. Kuimov, N. K. Gusarova, B. A. Trofimov, *Eur. J. Inorg. Chem.* **2012**, 4921 – 4929.
[33] Y. Wang, Y. Liu, Y. Zhang, F. Wang, P. J. Kowalski, H. W. Rohrs, R. A. Loomis, M. L. Gross, W. E. Buhro, *Angew. Chem.* **2012**, *124*, 6258 – 6261; *Angew. Chem. Int. Ed.* **2012**, *51*, 6154 – 6157.

